Aerosol Science and Technology

ISSN: 0278-6826 (Print) 1521-7388 (Online) Journal homepage: http://www.tandfonline.com/loi/uast20

The Relationship between Mass and Mobility for Atmospheric Particles: A New Technique for Measuring Particle Density

Peter H. McMurry , Xin Wang , Kihong Park & Kensei Ehara

To cite this article: Peter H. McMurry , Xin Wang , Kihong Park & Kensei Ehara (2002) The Relationship between Mass and Mobility for Atmospheric Particles: A New Technique for Measuring Particle Density, Aerosol Science and Technology, 36:2, 227-238, DOI: 10.1080/027868202753504083

To link to this article: http://dx.doi.org/10.1080/027868202753504083

Published online: 30 Nov 2010.

Submit your article to this journal

Article views: 1420

View related articles

Citing articles: 188 View citing articles

Full Terms & Conditions of access and use can be found at
http://www.tandfonline.com/action/journalInformation?journalCode=uast20

Download by: [University of North Texas] **Date:** 27 January 2017, At: 12:26

Aerosol Science and Technology 36: 227–238 (2002)
© 2002 American Association for Aerosol Research
Published by Taylor and Francis
0278-6826/02/$12.00 + .00

The Relationship between Mass and Mobility for Atmospheric Particles: A New Technique for Measuring Particle Density

Peter H. McMurry,[1] Xin Wang,[1] Kihong Park,[1] and Kensei Ehara[2]
[1]*Particle Technology Laboratory, Department of Mechanical Engineering, University of Minnesota, Minneapolis, Minnesota*
[2]*National Research Laboratory of Metrology, Umezono, Tsukuba, Ibaraki, Japan*

We describe a new technique for measuring the relationship between electrical mobility and mass. For spherical particles, the mass-mobility relationship can be used to determine particle density. For nonspherical particles, this relationship is affected by both the density and the dynamic shape factor; additional information would be required to determine either one. However, combinations of shape factors and densities that are consistent with measurements can be obtained. We show that the density of spherical particles of known composition can be measured to within ~5% with this approach. We applied the technique to urban atmospheric aerosols of ~0.1 and ~0.3 μm in Atlanta, GA, during August 1999. The Atlanta data show that particles of a given mobility often have several distinct masses. Based on complementary measurements, we argue that the most abundant mass consists of spherical hygroscopic particles. The measured mass for these particles (assuming that they are spherical) fell into the range of 1.54 to 1.77 g cm^{-3} at 3–6% relative humidity, which agreed to within about 5% of values calculated based on the measured size-resolved composition. Particles that were more and less massive than these were also observed. The less massive particles had "effective densities" of 0.25–0.64 g cm^{-3} and the more massive particles had "effective densities" of 1.7–2.2 g cm^{-3}. We hypothesize that the less massive particles consist of chain agglomerate soot.

Received 22 November 2000; accepted 28 February 2001.
Although the research described in this article has been funded wholly or in part by the United States Environmental Protection Agency through grant number R 826372-01-0 to the Georgia Institute of Technology and GIT subcontract number G-35-W62-G1 to the University of Minnesota, it has not been subjected to the Agency's required peer and policy review and therefore does not necessarily reflect the views of the Agency and no official endorsement should be inferred. We thank Dennis Savoie and Hal Maring for providing us with the MOUDI data from Atlanta.
Address correspondence to Peter H. McMurry, Particle Technology Laboratory, Department of Mechanical Engineering, University of Minnesota, 111 Church Street SE, Minneapolis, MN 55455. E-mail: mcmurry@me.umn.edu

INTRODUCTION

Density is an important property of aerosol particles. For example, density is required to determine the relationship between Stokes and aerodynamic diameters and to convert measured number distributions to mass distributions. Nevertheless, because few techniques are available to measure density, few measurements have been reported. The usual approach for determining density is to calculate it from measured aerosol composition. This can be problematic, however. It is often difficult to adequately characterize the composition of chemically complex aerosols, such as those found in the atmosphere. For example, organic compounds often make up a significant portion of the fine particles in the atmosphere but only a small fraction of these compounds can be identified. Due to the expense and expertize required, even these incomplete measurements are not done routinely. Therefore when density is calculated from measured composition, unverifiable assumptions are made regarding the properties of the organics. Furthermore, it is now well known that particles of a given size are typically externally mixed. It follows that densities are likely to vary with size and among particles of a given size, and it is important to understand those variabilities.

Several approaches for measuring density have been reported. Hänel and Thudium (1977) inferred the density of bulk dry atmospheric aerosol samples from independent measurements of volume and mass. Volume was found using a specially designed gas pycnometer. In 10 measurements of aerosols in Mainz, Jungfraujoch, Mace Head, and Deuselbach they found densities ranging from 1.8 g cm^{-3} to 3 g cm^{-3} with an average uncertainty of about 5%. Two to ten days were required to collect these samples. Because aerosol composition was not measured, it was not possible to compare measured with expected density. Kousaka et al. (1981) compared several methods for measuring the density of spherical aerosol particles. One of these techniques was applicable to the sub-0.5 μm diameter range of interest to us. Measurements involved the direct measurement of mass (e.g., with a piezo-electric mass monitor) and the measurement of particle

volume by integration over the size distributions measured with a differential mobility analyzer (DMA). Densities of polydisperse Diociyl Phthalaie (DOP) aerosols in two measurements were 5% and 10% greater than the true density. Stein et al. (1994) used the DMA-impactor technique developed by Kelly and McMurry (1992) to measure the density of 0.1 to 0.25 μm atmospheric particles in Meadview, AZ. They found that measured densities ranged from 1.60 to 1.79 g cm^{-3} and tended to decrease with increasing relative humidity. Estimated uncertainties were 4%, but measured densities were significantly higher than the value of 1.48 g cm^{-3} that was estimated from measurements of composition obtained with a cascade impactor. Hering and Stolzenburg (1995) and Sleicher et al. (1995) also reported on density measurements with variations of the DMA-impactor technique. These studies both focused on laboratory generated aerosols in the sub-50 nm diameter range. An important aspect of the Sleicher et al. work was the inference of fractal dimensions for irregularly shaped agglomerate particles.

This paper describes a new approach for measuring particle density. The technique involves first selecting particles of a known electrical mobility with a DMA (Liu and Pui 1974; Knutson and Whitby 1975) and then measuring their mass using Ehara's aerosol particle mass analyzer (APM; Ehara et al. 1996). For spherical particles, the electrical mobility equivalent diameter equals the geometric diameter. Density is determined from a knowledge of the geometric diameter and the mass. While true material density cannot be obtained for nonspherical particles, these measurements provide informative constraints on dynamic shape factors and densities.

We carried out laboratory experiments to verify the accuracy of measurements made with the DMA-APM technique. We also conducted measurements of urban aerosols during the intensive EPA Supersite study in Atlanta in August 1999. Measurements of size-resolved aerosol chemical composition were made in Atlanta, and we have used these data to test for closure between measured and calculated densities.

EXPERIMENT

Apparatus and Measurement Principles

A schematic of our apparatus is shown in Figure 1. We used a tandem differential mobility analyzer (TDMA; McMurry and Stolzenburg 1989) to select particles of known size at a known relative humidity before sending them to the APM for mass measurement. The measurements described in this paper could have been made with a single DMA rather than the TDMA. The TDMA was used because it was available and set up for relative humidity control and automated data acquisition. Also, it is our plan for the future to measure the density of particles as a function of relative humidity, and the TDMA will be required for those measurements. The measurements reported in this paper were all made at low relative humidity (3–6%). The aerosol and sheath air were dried with Nafion driers as they entered DMA1. Dry compressed air provided the DMA2 sheath air.

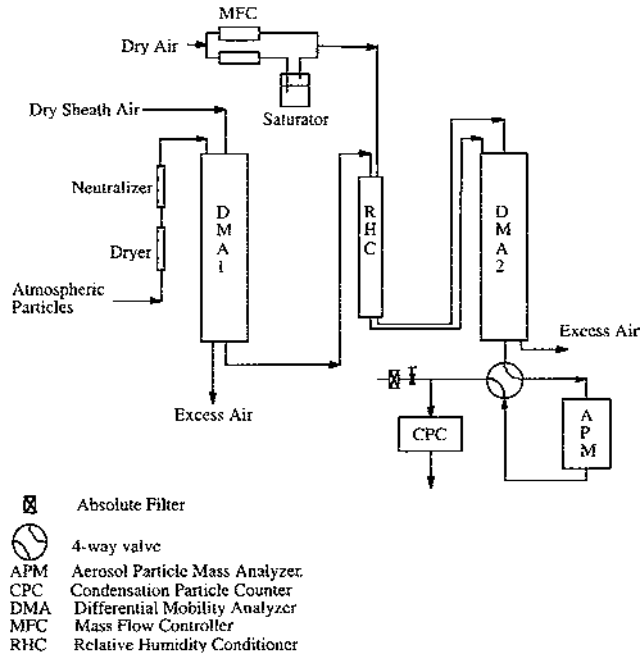

Figure 1. Schematic of experimental apparatus.

The DMA classifies particles according to electrical mobility, Z. For spherical particles, the electrical mobility equivalent diameter, d_{me}, equals the geometric or Stokes diameter and is independent of particle density. For nonspherical particles the electrical mobility depends on the dynamic shape factor, χ, which is defined by (e.g., Kasper 1982)

$$Z = \frac{neC_c(d_{me})}{3\pi\mu d_{me}} = \frac{neC_c(d_{ve})}{3\pi\mu d_{ve}\chi}, \qquad [1]$$

where n is the number of elementary charges per particle, e is the unit electric charge, C_c is the Cunningham slip correction factor (Allen and Raabe 1982), d_{me} is the mobility equivalent diameter, μ is the absolute viscosity of air, χ is the dynamic shape factor, and d_{ve} is the diameter of a sphere having the same volume as the irregularly shaped particle. For spherical particles $\chi = 1$ and $d_{me} = d_{ve}$, while for nonspherical particles $\chi > 1$ and $d_{me} > d_{ve}$. Note that the mobility equivalent diameter is independent of particle density.

The APM is described in detail by Ehara et al. (1996) and is illustrated in Figure 2. It consists of two 250 mm tall concentric cylinders that rotate together at a controlled rate about their common axis. The outer cylinder (63 mm internal radius) is maintained at ground, and a classifying voltage is applied to the inner cylinder (60 mm outer radius). The aerosol flows axially through this annular gap and rotates at the same angular velocity as the concentric cylinders. The particles experience radial electrical and centrifugal forces, which act in opposite directions. Particles will penetrate through the rotating cylinders to the downstream detector when these forces are equal. The

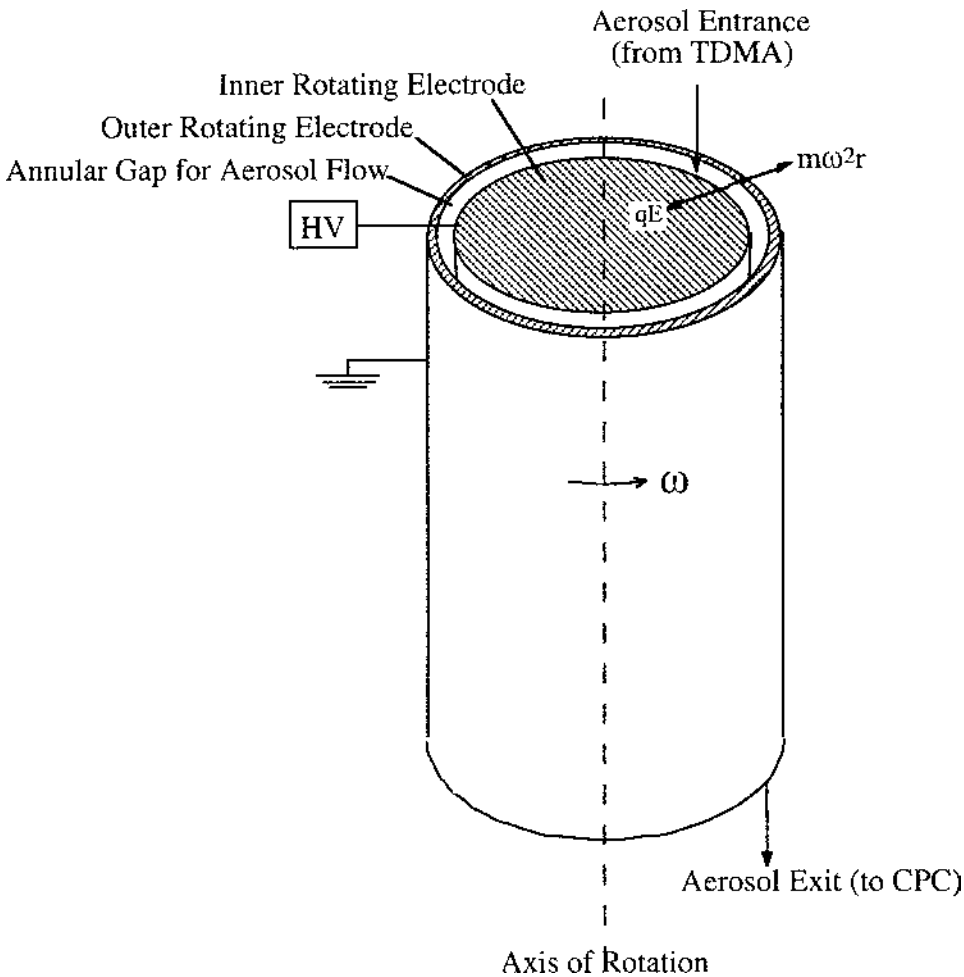

Figure 2. Schematic of APM.

equation that describes this force balance is

$$m\omega^2 r = \frac{\pi d_{ve}^3}{6}\rho_{\text{true}}\omega^2 r = neE_{\text{APM}}, \qquad [2]$$

where m is particle mass, ω is the APM rotational speed, ρ_{true} is the true material density of the particles, r is the radial distance to the annular gap from the axis of rotation, and E_{APM} is the magnitude of the electric field in the annular gap. Note that E_{APM} varies in proportion to the voltage applied to the inner cylinder, V_{APM}. Because the width of the annular gap is small compared to r, it is reasonable to assume, as an approximation, that E_{APM} and r are constant within the gap. Because centrifugal force varies in proportion to mass and is independent of shape, the relationship between d_{ve} and V_{APM} is independent of shape.

Aerosols are brought to Boltzmann equilibrium before they enter the system, so most particles will be singly charged ($n = 1$) if measurements are confined to sufficiently small sizes. The parameters ω, r, and E are also known. It follows that particle mass can be determined from Equation (2). For spherical particles ($\chi = 1$), d_{ve} is obtained from Equation (1) and density can then be obtained from Equation (2). Densities obtained in this way vary in proportion to d_{ve}^3. A small error in the diameter inferred from electrical mobility leads to a much larger error in density. For this reason we measured density by carrying out sequential measurements with polystyrene (PSL) spheres and the "unknown" aerosol under investigation (e.g., laboratory aerosols of known composition or atmospheric aerosols). The TDMA flow rates and classifying voltage were held fixed for the PSL and "unknown" aerosol to ensure that the mobility equivalent sizes were the same. Although there might be a small error in the absolute value of the mobility equivalent size, the relative sizes of the PSL spheres and the mobility equivalent diameter of the unknown particles should be equal to within about 1%. The APM rotational speed is held fixed while measuring the PSL and test particles. The true material density of the "test" aerosol, ρ_{test}, is then obtained by

$$\frac{m_{\text{test}}\omega^2 r}{m_{\text{PSL}}\omega^2 r} = \frac{\rho_{\text{true}}(\pi d_{ve}^3/6)}{\rho_{\text{PSL}}(\pi d_{\text{PSL}}^3/6)} = \frac{neE_{\text{APM test}}}{neE_{\text{APM PSL}}} = \frac{V_{\text{APM test}}}{V_{\text{APM PSL}}}. \qquad [3]$$

If test particles are spherical, $d_{ve\ \text{unknown}} = d_{me\ \text{unknown}} = d_{\text{PSL}}$ and the density of the "test" aerosol is

$$\rho_{\text{true (sphere)}} = \rho_{\text{PSL}} \frac{V_{\text{APM test}}}{V_{\text{APM PSL}}}. \quad [4]$$

The manufacturer gives a density of 1.054 g cm^{-3} for PSL spheres. The accuracy of this approach was determined using spherical laboratory-generated liquid test aerosols of known density, as is discussed in the experimental section. For irregularly shaped particles, we define the "effective density" of particles as

$$\rho_{\text{eff}} = \rho_{\text{PSL}} \frac{V_{\text{APM test}}}{V_{\text{APM PSL}}} = \rho_{\text{true}} \frac{d_{ve}^3}{d_{me}^3}. \quad [5]$$

Because $d_{me} > d_{ve}$ for nonspherical particles, the densities of nonspherical particles calculated in this way are less than the true material densities. If the shape factor is known, then d_{ve} can be obtained from Equation (1) and the true material density can be determined. It is important to point out that the "effective density" measured with the DMA impactor technique (Kelly and McMurry 1992) is identical to the value obtained with the DMA-APM.

The previous discussion assumed that particles carry a single elementary charge ($n = 1$). Particles of a given mobility selected by the DMA typically contain both singly and multiply charged particles. The APM classifies particles according to a mass-to-charge ratio, which varies as d_{ve}^3/n while the DMA classifies particles according to $(d_{me}^p)/n$ $(1 < p < 2)$. In this paper our measurements are done using particles having mobility equivalent sizes of 0.107 and 0.309 μm. For these sizes, the APM voltages required to classify doubly charged particles of a given density and mobility are, respectively, 1.94 and 2.48 times the values required to classify singly charged particles. It follows that multiply charged particles of a given mobility are cleanly separated by the APM.

RESULTS AND DISCUSSION

In this section we describe measurements of particle density for atmospheric aerosols and well-characterized laboratory aerosols. The laboratory studies were done to assess the accuracy of our measurement protocol. The atmospheric measurements were done in Atlanta during August, 1999, and involved the same protocol used in the laboratory. Measurements were done for particles of nominal mobility-equivalent diameters of 0.107 and 0.309 μm. These sizes were used because PSL spheres of these sizes were available for reference (see Equation (4)); we plan to extend measurements to smaller and larger sizes in the future. Table 1 summarizes the DMA 1 and DMA 2 sheath and aerosol flow rates as well as the aerosol flow rate through the APM for these measurements.

Laboratory Studies

The accuracy of densities for spherical particles obtained with Equation (4) was determined by using test aerosols of dioctyl sebacate (DOS; $\rho = 0.915$ g cm^{-3}) and Fomblin Y-25, a diffusion pump oil with density that we measured to be 1.886 $\pm$ 0.005 g cm^{-3}. These substances were used because they produce spherical liquid droplets, they have very low vapor pressures and will therefore not evaporate appreciably during transport through the TDMA-APM apparatus, and they cover the range of densities pertinent to submicron atmospheric particles. Polydisperse test aerosols were generated from 0.1 volume percent solutions of the DOS or Fomblin in 99.7+% HPLC grade 2 propanol with a Collison atomizer.

The experimental procedure involved first measuring the PSL penetration through DMA1 as a function of the DMA1 classifying voltage. The DMA1 voltage was set at the value that provided maximum penetration, and the DMA2 voltage that provided maximum penetration was then determined. With the DMA1 and DMA2 classifying voltages set at these values, the penetration through the APM was measured as a function of the APM classifying voltage. An example of these measurements is shown in Figure 3. Also shown in Figure 3 is the penetration of Fomblin through the TDMA-APM system as a function of APM classifying voltage. The peak penetration for the Fomblin occurred at an APM classifying voltage of 140.4 V, while the corresponding values for PSL was 79.8 V. It follows from Equation (4) that the measured density for Fomblin was 1.85 g cm^{-3}, which is 1.9% below the expected value. A summary of all laboratory measurements for DOS and Fomblin are given in Table 2. Density measurements for these species were repeated on different days for each particle size. DOS densities were typically within 5% of the expected value, while Fomblin densities were within 2%. We conclude that sequential measurements of PSL and the test aerosol enable measurements of densities for spherical particles to within ~5%. If densities had been obtained directly from the DMA size and the APM mass, it is likely that accuracies would

Table 1
TDMA and APM flow rates for 0.107 and 0.309 μm measurements

D_p, μm	DMA1 inlet and outlet sheath airflow rate, LPM	DMA1 inlet and outlet aerosol flow rate, LPM	DMA2 inlet and outlet sheath airflow rate, LPM	DMA2 inlet and outlet aerosol flow rate, LPM	APM flow rate, LPM
0.107	10.6	1.47	6.91	1.49	1.49
0.309	5.0	0.50	3.05	0.50	0.50

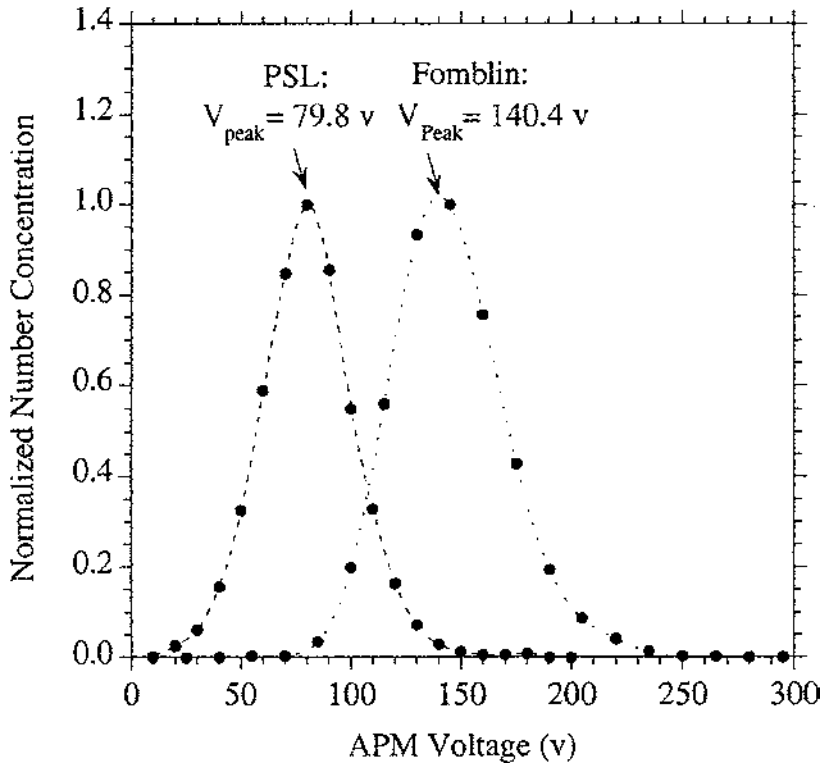

Figure 3. Normalized concentration downstream of APM versus APM classifying voltage for PSL spheres and Fomblin aerosols of the same mobility equivalent diameter (~0.309 μm diameter).

have been about a factor to two worse than this since, even with very careful attention to flows and voltage calibrations, the absolute accuracy with which size can be obtained with the DMA is about 3% (Kinney et al. 1991).

Measurements on Urban Atlanta Aerosols

Using the experimental procedures described above, we carried out 11 TDMA-APM measurements of 0.107 μm atmospheric aerosols and 10 measurements of 0.309 μm aerosols. The results of these measurements are summarized in Table 3 and are discussed below. The "effective densities" shown in Table 3 and in the figures were calculated using Equation (5).

Table 2
Summary of density measurements with laboratory-generated particles

	Measured density, g cm^{-3}	Error,%
Fomblin		
0.309 μm	1.83	−3.0
0.309 μm	1.82	−3.6
0.107 μm	1.85	−1.9
0.107 μm	1.85	−1.7
DOS		
0.309 μm	0.87	−4.5
0.309 μm	0.86	−5.8
0.107 μm	0.95	+3.8
0.107 μm	0.95	+3.8

Figure 4 shows the penetration of 0.107 μm PSL and atmospheric particles through the APM as a function of APM classifying voltage on the afternoon of August 3, 1999. Note that a single peak is observed for the atmospheric particles, suggesting that on this day all particles of a given mobility had the same mass. The effective density of these particles is 1.61g cm^{-3}.

Figure 5 shows the penetration of 0.309 μm PSL and atmospheric particles through the APM on the morning of August 10, 1999. In this case distinct peaks are observed at 67 V and 246 V. The effective densities calculated from Equation (4) for these peaks are 0.44 g cm^{-3} and 1.62 g cm^{-3}. It is highly unlikely that atmospheric particles could have a material density as small as 0.44 g cm^{-3}. We pointed out above that the densities of nonspherical particles obtained in this way would be smaller than the true material densities. We therefore hypothesize that the low mass particles in Figure 5 were porous or nonspherical. We did not collect samples for analysis by electron microscopy in this study. However, previous work has shown that urban atmospheric particles in this size range often include carbon-rich chain agglomerates (e.g., McMurry et al. 1996) similar to those that are observed in sooty emissions from diesel engines, etc.

Table 3
Summary of APM measurements, Atlanta, GA, August 1999

Date	V_{psl}, v	V_{atm1}, v	V_{atm2}, v	V_{atm3}, v	V_{atm4}, v	ρ_{eff1}, g cm^{-3}	ρ_{eff2}, g cm^{-3}	ρ_{eff3}, g cm^{-3}	ρ_{eff4}, g cm^{-3}	N_1, cm^{-3}	N_2, cm^{-3}	N_3, cm^{-3}	N_4, cm^{-3}	d_{ae1} μm
0.309 μm														
8/4/99 12–15	165	39	241	270	300	0.249	1.54	1.72	1.92	0.6	2.5	2.4	1.7	0.118
8/5/99 8–10	170	60	255	305	360	0.372	1.58	1.89	2.23	1.3	4.1	3.3	1.7	0.160
8/6/99 15–16	160	65	269	—	—	0.428	1.77	—	—	0.1	0.7	—	—	0.176
8/6/99 16–19	160	60	250	—	330	0.395	1.65	—	2.17	0.1	1.2	—	0.8	0.167
8/7/99 19–21	163	60	249	—	—	0.388	1.61	—	—	0.1	1.0	—	—	0.164
8/9/99 15–16	165	57	262	300	—	0.364	1.67	1.92	—	0.1	0.8	0.6	—	0.157
8/10/99 9–11	160	67	246	—	—	0.441	1.62	—	—	0.5	0.6	—	—	0.180
8/10/99 20–21	160	55	241	—	300	0.362	1.59	1.84	1.98	0.2	0.6	—	0.3	0.157
8/11/99 10–11	162	70	250	—	—	0.455	1.63	—	—	0.3	0.6	—	—	0.184
8/12/99 12–13	159	69	235	—	—	0.457	1.56	—	—	0.5	0.8	—	—	0.185
0.107 μm														
8/3/99 16–18	57	—	87	—	—	—	1.61	—	—	—	6.6	—	—	—
8/5/99 13–14	63	—	93	180	—	—	1.56	—	—	—	3.4	0.9	—	—
8/5/99 15–16	65	—	101	210	—	—	1.64	—	—	—	5.8	1.4	—	—
8/7/99 17–19	62	—	107	—	—	—	1.82	—	—	—	7.4	—	—	—
8/8/99 15–16	62	—	79	—	—	—	1.35	—	—	—	1.7	—	—	—
8/9/99 9–11	60	—	78	130	—	—	1.37	—	—	—	4.0	2.5	—	—
8/10/99 14–15	63	—	111	—	—	—	1.86	—	—	—	6.0	—	—	—
8/10/99 18–20	65	35	100	—	—	0.569	1.63	—	—	0.7	2.1	—	—	0.067
8/12/99 15–16	64	—	92	190	—	—	1.52	—	—	—	6.5	1.0	—	
8/13/99 10–11	66	40	100	—	—	0.641	1.60	—	—	5.0	11.0	—	—	0.075
8/14/99 9–10	68	—	104	—	—	—	1.62	—	—	—	11.0	—	—	—

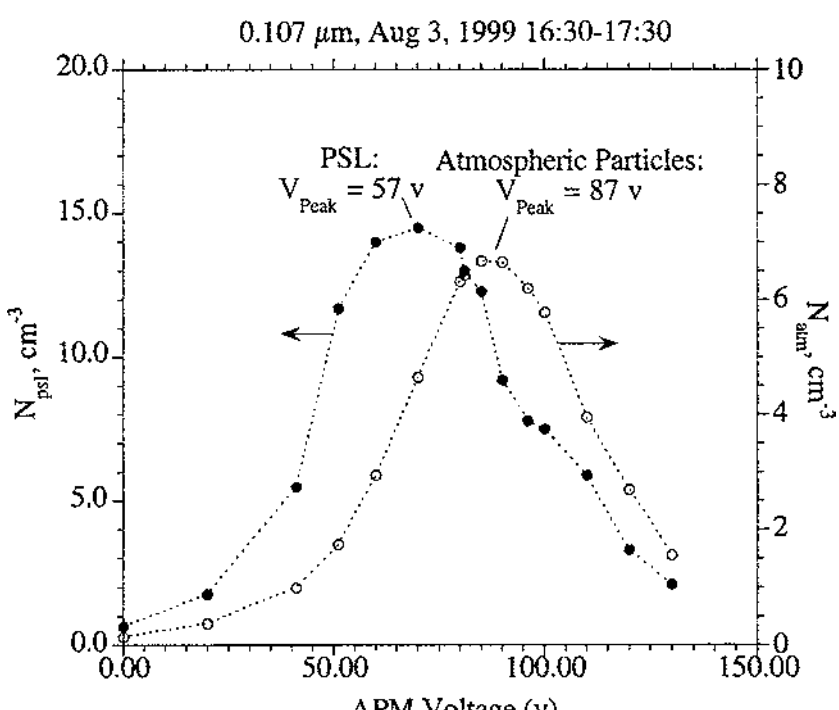

Figure 4. Concentration downstream of APM versus APM classifying voltage for PSL spheres and atmospheric particles of the same mobility equivalent diameter (0.107 μm). Only a single mass peak was observed for atmospheric particles on this day.

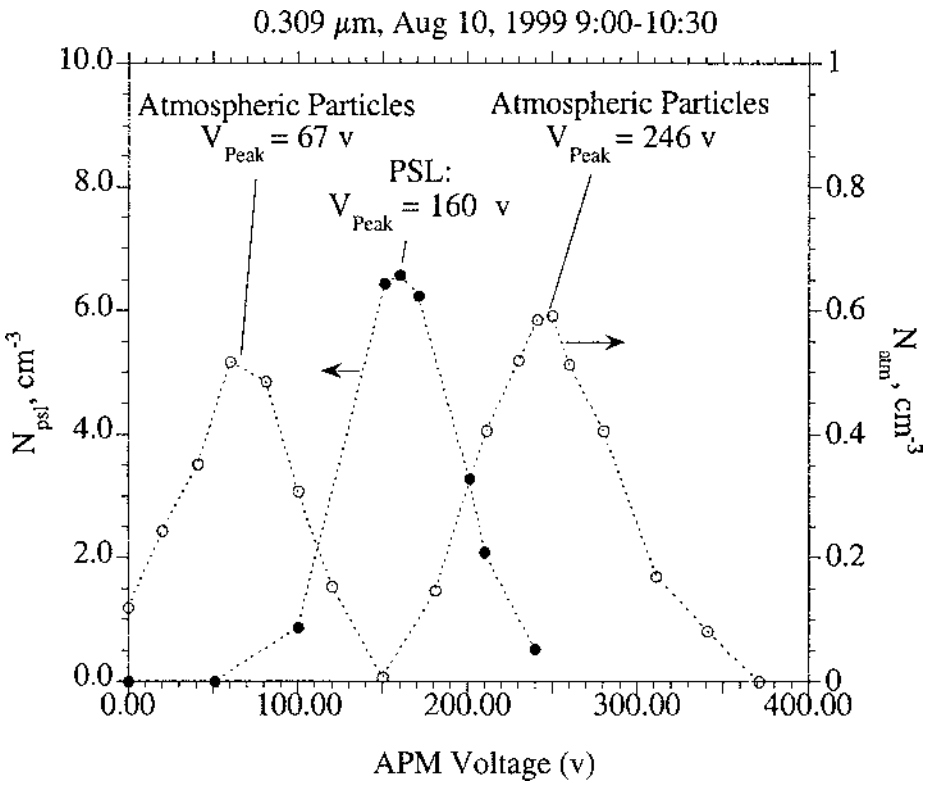

Figure 5. Concentration downstream of APM versus APM classifying voltage for PSL spheres and atmospheric particles of the same mobility equivalent diameter (0.309 μm). Two distinct mass peaks, one heavier and one lighter than PSL, were observed during this measurement.

A more complex APM spectrum for 0.309 μm particles is shown in Figure 6. The major peak ($V = 255$ V) corresponds to particles with a density of 1.58 g cm^{-3}, which is close to values seen in Figures 4 and 5. Also, low-mass particles with an effective density of 0.37 g cm^{-3} were observed, although in a lower proportion than is seen in Figure 5. Also observed in Figure 6 are "shoulders" at 305 V and 360 V. Doubly charged particles of 0.37 g cm^{-3} and 1.58 g cm^{-3} would have been classified at APM voltages of 149 V and 422 V, respectively. We conclude that these shoulders correspond to more massive particles that would have densities of 1.89 and 2.23 g cm^{-3} if they were spherical. Direct measurement of composition would be required to establish their identities.

We routinely measured water uptake of 0.107 μm and 0.309 μm particles immediately prior to or after we measured density with the TDMA-APM. We found that, on average, 83% of the 0.309 particles and 79% of the 0.107 μm particles were "more hygroscopic," while the remainder absorbed only a small amount of water when humidified. Figure 7 shows that there is a relationship between the less massive or "fluffy" fraction separated with the APM and the "less hygroscopic" fraction separated with the TDMA for 0.309 μm particles measured on the same day. This observation suggests that the "more hygroscopic" particles correspond to the more massive particles separated with the APM. Furthermore, because the "less massive" and "less hygroscopic" particles were present in similar proportions, and because previous work in Minneapolis showed that the "less hygroscopic" particles contained carbon-rich chain-agglomerates, we hypothesize that the particles with effective densities <1 g cm^{-3} are chain agglomerate soot particles. Because the APM did not separate the low density particles as cleanly at 0.107 μm (see discussion on Figure 8 below), this argument cannot be extended to the smaller size. Nevertheless, the TDMA measurements showed that "less hygroscopic" particles were always found at 0.107 μm, suggesting that low density particles were present but were not cleanly separated by the APM.

Although it is not possible to determine the true density for nonspherical particles using the TDMA-APM technique, values of d_{ve} that are consistent with measurements can be found from Equation (1) for assumed values of the dynamic shape factor, χ. Values of the true material density, ρ_{true}, that are consistent with these values of d_{ve} and χ can then be found from Equation (3). These calculated relationships between ρ_{true} and χ for all of the low density particles measured in Atlanta are shown in Figure 8. Note that low density particles were observed in all 10 measurements at 0.309 μm but for only 2 of the 11 measurements at 0.107 μm. The data in Figure 8 show that for a given true material density, the shape factors for 0.107 μm particles are smaller than

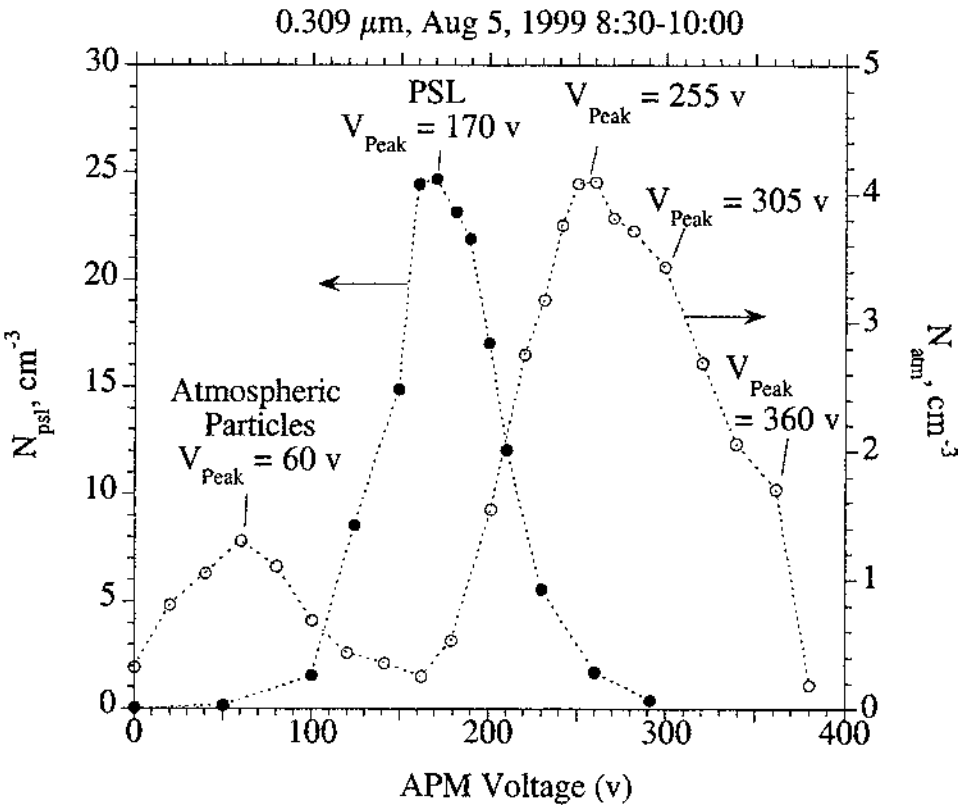

Figure 6. Concentration downstream of APM versus APM classifying voltage for PSL spheres and atmospheric particles of the same mobility equivalent diameter (0.309 μm). Evidence for four mass peaks is apparent from this measurement.

for 0.309 μm particles. This suggests that the smaller particles are more "compact" and are therefore not so easily separated from particles of other types by the APM. It is often argued that chain agglomerate soot consists of amorphous carbon, which has a density of $\sim$2 g cm^{-3}. If this is true, then the shape factors for the low density 0.309 μm particles range from 2.1 to 2.8,

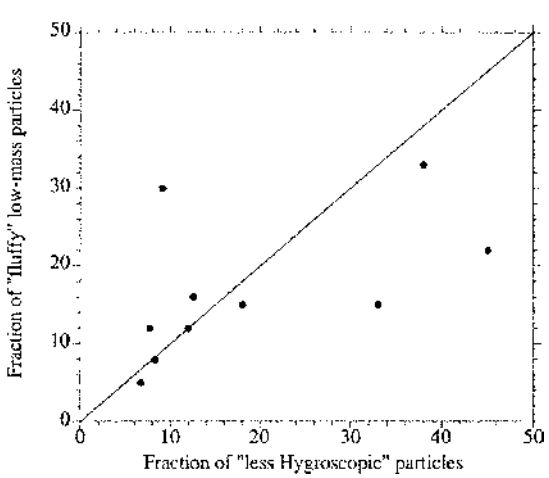

Figure 7. Fraction of particles with effective densities <1 g cm^{-3} versus fraction of "less hygroscopic" particles measured with the TDMA in sequential measurements.

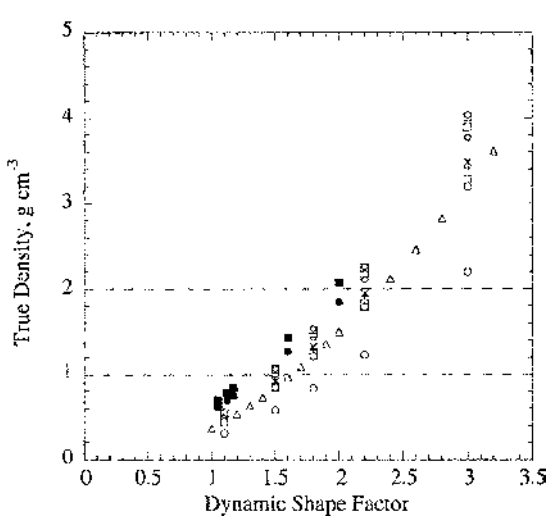

Figure 8. Relationship between the true material density and the dynamic shape factor for the low mass (effective density <1 g cm^{-3}) particles. The open symbols are for 0.309 μm particles and the closed symbols are for 0.107 μm particles. The horizontal dashed lines cover the range of densities that might be anticipated for carbon soot.

while the corresponding values for 0.107 μm particles is 1.8 to 2.1. If the true density is 1 g cm^{-3}, the shape factors would range from 1.5 to 2.1 for 0.309 μm particles and from 1.2 to 1.5 for 0.107 μm particles.

A limited amount of information on shape factors and "effective density" of soot is available from previous studies. Odumade (1983) measured the dynamic shape factors of chain agglomerate particles generated by a propane flame. He used an electron microscope to measure the spherical equivalent volume of individual chain agglomerate particles selected according to electrical mobility with a DMA. Measurements were done with particles ranging from 0.1 to 0.15 μm mobility equivalent size. Dynamic shape factors calculated with Equation (1) for 25 particles were 1.49 ± 0.33, which is in the range of values we found for 0.107 μm particles. There is no assurance, however, that Odumade's aerosols had similar morphologies to the atmospheric particles sampled in our study. Ahlvik et al. (1998) found "effective densities" for diesel soot with the DMA-impactor technique. They found that these effective densities decreased with increasing size, and were equal to $\sim$1.4 g cm^{-3} and $\sim$ 0.6 g cm^{-3} for particles of $\sim$ 0.1 μm and 0.3 μm, respectively. These values are significantly higher than the values we measured (see Table 3).

We also calculated the aerodynamic diameter for the low density particles so as to estimate how they would be classified by an inertial impactor. The relationship between aerodynamic diameter; d_{ae}, and mobility equivalent diameter is

$$d_{ae}^2 C(d_{ae}) = \frac{1}{\chi}\frac{\rho_{\text{true}}}{\rho_0} d_{ve}^2 C(d_{ve}) = \frac{\rho_{\text{eff}}}{\rho_0} d_{me}^2 C(d_{me}). \qquad [6]$$

Values of d_{ae} for our Atlanta measurements are shown in Table 3. Note that aerodynamic diameters range from 38% to 75% of the mobility equivalent size.

We did not measure the composition of particles in the various APM mass peaks. However, in all measurements we found a major peak with density in the range of 1.6 g cm^{-3} (see columns labeled ρ_{atm2} in Table 3). We have compared the densities of these major peaks with densities of the ambient aerosol during our sampling period estimated from the measured size-resolved compositions measured with MOUDI impactors by Savoie and coworkers at the University of Miami. Assuming that species volumes do not change upon mixing, the density of an internally mixed particle is

$$\rho_{\text{true atm}} = \frac{\sum_{\text{species}} m_i}{\sum_{\text{species}} \frac{m_i}{\rho i}} = \frac{\sum_{\text{species}} c_i}{\sum_{\text{species}} \frac{c_i}{\rho i}} = \frac{1}{\sum_{\text{species}} \frac{f_i}{\rho i}}, \qquad [7]$$

where m_i and c_i are the mass and mass concentration of species i associated with particles in the size range of interest and f_i is the mass fraction of species i. Values of f_i obtained from the MOUDI data are given in Table 4. Two MOUDI samples were obtained daily (nominally 7:30 a.m. or p.m. to 6 p.m. or a.m.; data from the closest available sampling period to the APM measurements was used to estimate f_i). For composition of 0.107 μm particles we used MOUDI data from the 0.098–0.18 μm aerodynamic diameter MOUDI stage, while for the 0.309 μm particles we used data from the 0.18–0.32 μm aerodynamic diameter stage. Values of species densities, ρ_i, used in these calculations are given in Table 4. The assumed value for Organic Carbon (OC) density (1.2 g cm^{-3}) is based on the recommendation of Turpin and Lim (2000). We assume that all nitrate is in the form of ammonium nitrate and that the balance of the ammonium is with the sulfate. The ammonium-to-sulfate molar rations, B, then range from 1.15 to 2.05. The sulfates are assumed to consist of a mixture of ammonium bisulfate (NH_4HSO_4) and letovicite ($(NH_4)_2H(SO_4)_2$) if the ammonium to sulfate ratio is between 1.0 and 1.5 and a mixture of letovicite and ammonium sulfate ($(NH_4)_2SO_4$) if the ammonium-to-sulfate ratio is between 1.5 and 2.0. Because our measurements were made at relative humidities in the 3% to 6% range, which is well below the efflorescence relative humidity for these compounds (Spann and Richardson, 1985), we assume that particles contain no water.

Densities calculated with Equation (7) are compared with measured values (ρ_{atm2}) in Figures 9a and b. In making these comparisons we have implicitly assumed that particles are spherical, that they contain no water, and that their composition is given by Table 4. We believe these are reasonable but not perfect assumptions. It is quite likely that some of the species in Table 4 are associated with other mass peaks. For example, it may be that EC is more likely associated with the "fluffy" (peak 1) particles than the peak 2 particles. However, excluding EC from these calculations would not have a large effect on calculated densities, since f_{EC} is typically fairly small. Also, TDMA measurements for water uptake show that a small amount of water uptake is typically observed even at very low humidities (see Figure 10). This would tend to suggest that particles probably contain very little water, but that they contain enough liquid to be spherical. The fact that the "more hygroscopic" particles absorb some water at the very low humidities where APM measurements were carried out does not necessarily contradict our assumption that the inorganics were crystalline solids. Based on our previous work, we believe that OC is responsible for water uptake at low relative humidities (Dick et al. 2000).

The time series comparisons in Figures 9a and b show reasonable agreement between measured and calculated densities. On average, the absolute percentage differences between calculated and measured densities are 5% $\pm$ 5% for 0.107 μm particles and 4% $\pm$ 3% for 0.309 μm particles, which are comparable to the accuracy of the density measurement technique. Perfect agreement would not be expected even if the density measurements were perfect since the MOUDI measurements extend over a longer sampling period than the APM measurements. Of particular interest is the low density measured at 0.107 μm on September 8, 1999. The calculated density on this date was also low since particles of $\sim$0.1 μm were unusually rich in OC.

Table 4
Fractional mass concentrations of major aerosol species during TDMA-APM measurements, and calculated particle densities

	$f_{SO_4^=}$	$f_{NO_3^-}$	$f_{NH_4^+}$	f_{OC}	f_{EC}	ρ_{calc}, g cm^{-3}
0.309 μm APM measurements						
8/4/1999 12–15	0.56	0.00	0.17	0.21	0.05	1.65
8/5/1999 8–10	0.54	0.00	0.18	0.22	0.05	1.63
8/6/1999 15–16	0.47	0.00	0.15	0.21	0.17	1.65
8/6/1999 16–19	0.47	0.00	0.15	0.21	0.17	1.65
8/7/1999 19–21	0.36	0.00	0.13	0.41	0.10	1.50
8/9/1999 15–16	0.64	0.00	0.14	0.15	0.07	1.68
8/10/1999 9–11	0.48	0.00	0.12	0.29	0.11	1.59
8/10/1999 20–21	0.36	0.00	0.13	0.40	0.11	1.51
8/11/1999 10–11	0.54	0.00	0.17	0.19	0.10	1.67
8/12/1999 12–13	0.36	0.00	0.14	0.30	0.20	1.58
0.107 μm APM measurements						
8/3/1999 16–18	0.19	0.00	0.06	0.60	0.14	1.42
8/5/1999 15–16	0.44	0.00	0.15	0.32	0.09	1.57
8/5/1999 13–14	0.44	0.00	0.15	0.32	0.09	1.57
8/7/1999 17–19	0.53	0.00	0.12	0.27	0.08	1.60
8/8/1999 15–16	0.17	0.00	0.00	0.75	0.08	1.25
8/9/1999 9–11	0.44	0.00	0.13	0.29	0.14	1.60
8/10/1999 14–15	0.31	0.00	0.10	0.35	0.25	1.57
8/10/1999 18–20	0.31	0.00	0.10	0.35	0.25	1.57
8/12/1999 15–16	0.26	0.00	0.08	0.37	0.30	1.56
8/13/1999 10–11	0.26	0.00	0.09	0.37	0.27	1.55
8/14/1999 9–10	0.60	0.00	0.16	0.19	0.05	1.67

The TDMA and APM data also enable us to estimate the dependence of aerodynamic diameter on relative humidity for the more hygroscopic fraction. Typical results for 0.107 and 0.309 μm particles are shown in Figure 11. In order to obtain the aerodynamic diameters shown in Figure 11 it was necessary to have estimates of relative humidity dependent density. We assumed that at 0% relative humidity the particle density equals ρ_{eff2} from Table 3. Densities at higher humidities were calculated by assuming that the increase in mobility equivalent size with relative humidity was due solely to uptake of water and that the volume of mixing was zero (Dick et al. 2000). Note from Figure 11 that aerodynamic diameter is less sensitive to relative humidity than is volume equivalent (mobility equivalent diameter). This is because the decrease in density that occurs as particles absorb water compensates to some extent for the increase in particle size. Note also that for these data, aerodynamic sizes at 70% relative humidities are 3–4% larger than the dry particle size and are 12–16% larger at 80% relative humidity. The sensitivity of aerodynamic diameter to relative humidity increases sharply at higher humidities due to the rapid uptake of water and the tendency of densities to approach that of water. This reinforces our previous argument that sampling with impactors should be done at relative humidities below 80% (Vasiliou et al. 1999).

Table 5
Species densities used to calculate density of atmospheric aerosols

Species	Density, g cm^{-3}
NH_4NO_3	1.72
NH_4HSO_4	1.78
$(NH_4)_3H(SO_4)_2$	1.83
$(NH_4)_2SO_4$	1.77
OC	1.2
EC	2.0

CONCLUSIONS

A new technique for measuring the density of gas-borne particles is reported. The technique involves using Ehara's APM to measure the mass of particles that have been classified according to electrical mobility with a DMA. With this technique the density of spherical particles in the 0.1 to 0.3 μm diameter range can be measured to within 5%. Due to a malfunction of the instrument during the field study we did not obtain measurements outside this range. However, according to the manufacturer the APM can classify unit density particles as small as 20 nm and the technique could also be extended to particles larger than 0.3 μm. For nonspherical particles these measurements provide

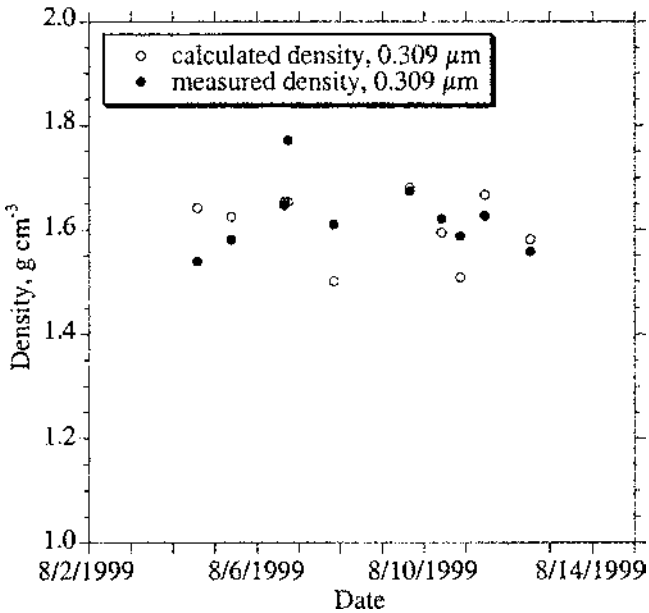

(*a*)

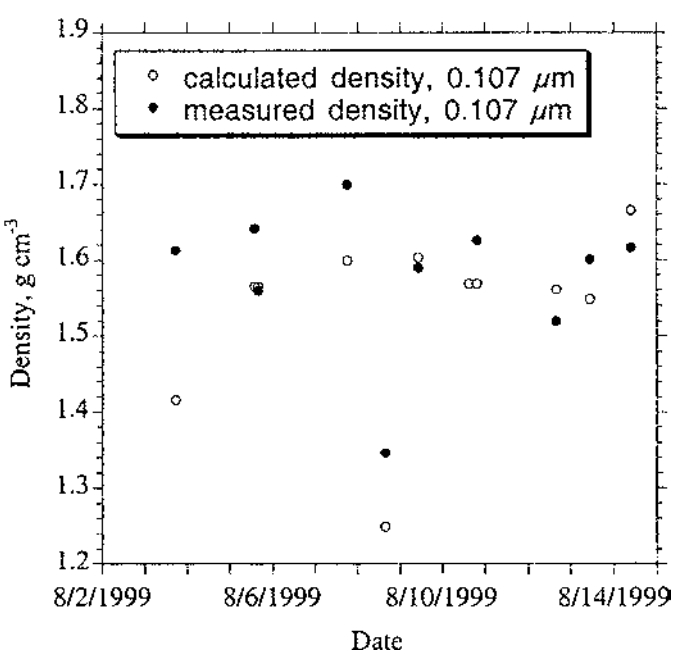

(*b*)

Figure 9. Time series comparison of calculated and measured densities for the major mass peak for 0.309 μm (a) and 0.107 μm (b) particles in Atlanta.

combinations of particle density and dynamic shape factors that are consistent with observations.

We applied this technique to 0.1 μm and 0.3 μm urban Atlanta, GA, aerosols during the EPA Supersite study in August 1999. We found that particles typically included a major mass peak with a density in the ~1.5 to 1.7 g cm^{-3} range at

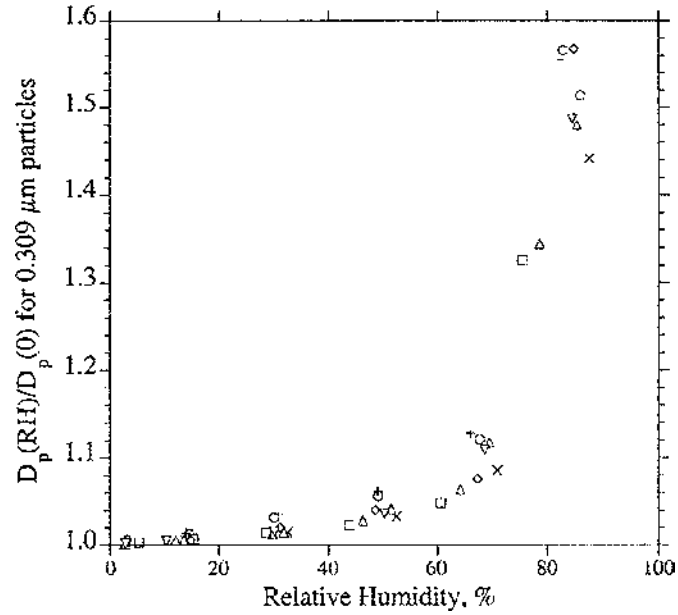

Figure 10. Diameter growth factors for "more hygroscopic" 0.309 μm particles measured with the TDMA at about the same time that APM density measurements were done.

3–6% relative humidity. These densities agreed with calculated densities, based on the measured size-resolved composition, to within about 5%. The data provide clear evidence, however, that singly charged particles of a given electrical mobility contain several distinct masses. Very low mass particles with "effective densities" in the 0.35 to 0.65 g cm^{-3} range were often observed. We hypothesize that these particles may consist of chain agglomerate soot. Some measurements provide evidence for

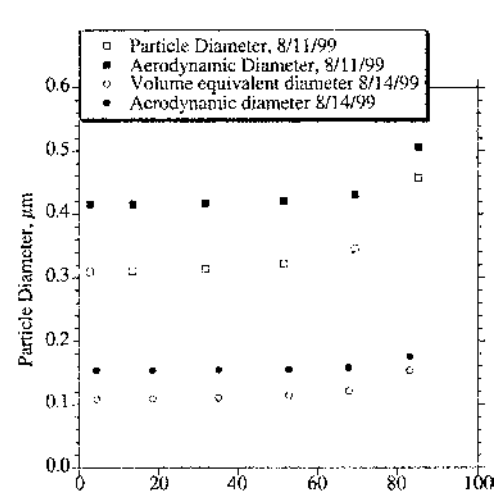

Figure 11. Measured volume-equivalent diameters and calculated aerodynamic diameters for more hygroscopic particles as a function of relative humidity for typical 0.309 and 0.107 μm data.

particles with "effective densities" in the 1.7 to 2.2 g cm^{-3} range. Further work is needed to identify the composition of those particles.

REFERENCES

Ahlvik, P., Ntziachristos, L., Keskinen, J., and Virtanen, A. (1998). *Real Time Measurements of Diesel Particle Size Distribution with an Electrical Low Pressure Impactor*, SAE International Congress and Exposition, SAE International, Detroit, MI.

Allen, M. D., and Raabe, O. G. (1982). Re-Evaluation of Millikan's Oil Drop Data for the Motion of Small Particles in Air, *J. Aerosol Sci.* 13(6): 537–547.

Dick, W. D., Saxena, P., and McMurry, P. H. (2000). Estimation of Water Uptake by Organic Compounds in Submicron Aerosols Measured during the Southeastern Aerosol and Visibility Study, *J. Geophy. Res.* 105(D1):1471–1479.

Ehara, K., Hagwood, C., and Coakley, K. J. (1996). Novel Method to Classify Aerosol Particles According to their Mass-to-Charge Ratio: Aerosol Particle Mass Analyser, *J. Aerosol Sci.* 27(2):217–234.

Hänel, G., and Thudium, J. (1977). Mean Bulk Densities of Samples of Dry Atmospheric Aerosol Particles: A Summary of Measured Data, *Pageoph*. 115:799–803.

Hering, S. V., and Stolzenburg, M. R. (1995). On Line Determination of Particle Size and Density in the Nanometer Size Range, *Aerosol Sci. Technol*. 23(2):155–173.

Kasper, G. (1982). Dynamics and Measurement of Smokes. I. Size Characterization of Nonspherical Particles, *Aerosol Sci. Technol*. 1:187–199.

Kelly, W. P., and McMurry, P. H. (1992). Measurement of Particle Density by Inertial Classification of Differential Mobility Analyzer-Generated Monodisperse Aerosols, *Aerosol Sci. Technol*. 17:199–212.

Kinney, P. D., Pui, D. Y. H., Mulholland, G. W., and Bryner, N. P. (1991). Use of Electrostatic Classification Method to Size 0.1 μm SRM Particles—A Feasibility Study, *J. Res. Natl. Stand. Technol*. 96(2): 147–176.

Knutson, E. O., and Whitby, K. T. (1975). Aerosol Classification by Electric Mobility: Apparatus, Theory, and Application, *J. Aerosol Sci.* 6:443–451.

Kousaka, Y., Okuyama, K., and Endo, S. (1981). Comparison Among Measuring Methods of Density of Spherical Aerosol Particles, *J. Chem. Eng. Japan* 14(3):214–218.

Liu, B. Y. H., and Pui, D. Y. H. (1974). A Submicron Aerosol Standard and the Primary, Absolute Calibration of the Condensation Nuclei Counter, *J. Colloid Interface Sci.* 47:155–171.

McMurry, P. H., Litchy, M., Huang, P. F., Cai, X. P., Turpin, B. J., Dick, W. D., and Hanson, A. (1996). Elemental Composition and Morphology of Individual Particles Separated by Size and Hygroscopicity with the TDMA, *Atmos. Environ.* 30(1):101–108.

McMurry, P. H., and Stolzenburg, M. R. (1989). On the Sensitivity of Particle Size to Relative Humidity for Los Angeles Aerosols, *Atmos. Environ*. 23(2):497–507.

Odumade, O. (1983). Mobilities of Aggregates of Particles, *Mechanical Engineering*, Ph.D. Dissertation, University of Minnesota Minneapolis, MN, 209.

Sleicher, B., Künzel, S., and Burtscher, H. (1995). In Situ Measurement of Size and Density of Submicron Aerosol Particles, *J. Appl. Phys.* 78(1):4416–4422.

Spann, J. F., and Richardson, C. B. (1985). Measurement of the Water Cycle in Mixed Ammonium Acid Sulfate Particles. *Atmos. Environ*. 19:819–826.

Stein, S. W., Turpin, B. J., Cai, X. P., Huang, C. P. F., and McMurry, P. H. (1994). Measurements of Relative Humidity-Dependent Bounce and Density for Atmospheric Particles Using the DMA-Impactor Technique, *Atmos. Environ*. 28(10):1739–1746.

Turpin, B. J., and Lim, H.-J. (2001). Species Contributions to $PM_{2.5}$ Mass Concentrations: Revisiting Common Assumptions for Estimating Organic Mass, *Aerosol Sci. Technol*. 35:602–610.

Vasiliou, J. G., Sorensen, D., and McMurry, P. H. (1999). Sampling at Controlled Relative Humidity with a Cascade Impactor, *Atmos. Environ*. 33(7):1049–1056.